Aqueous Humor Biomarkers Identify Three Prognostic Groups in Uveal Melanoma

Annemijn P. A. Wierenga,[1] Jinfeng Cao,[1,2] Henk Mouthaan,[3] Christiaan van Weeghel,[1] Robert M. Verdijk,[4,5] Sjoerd G. van Duinen,[4] Wilma G. M. Kroes,[6] Mehmet Dogrusöz,[1] Marina Marinkovic,[1] Sjoerd S. H. van der Burg,[7] Gregorius P. M. Luyten,[1] and Martine J. Jager[1]

[1]Department of Ophthalmology, Leiden University Medical Center, Leiden, The Netherlands
[2]Department of Ophthalmology, The Second Hospital of Jilin University, Changchun, China
[3]Olink Proteomics, Uppsala, Sweden
[4]Department of Pathology, Leiden University Medical Center, Leiden, The Netherlands
[5]Department of Pathology, Section Ophthalmic Pathology, Erasmus MC University Medical Center, Rotterdam, The Netherlands
[6]Department of Clinical Genetics, Leiden University Medical Center, Leiden, The Netherlands
[7]Department of Medical Oncology, Leiden University Medical Center, Leiden, The Netherlands

PURPOSE. To investigate whether we can identify different patterns of inflammation in the aqueous humor of a uveal melanoma (UM)-containing eye, and whether these are related to prognosis.

METHODS. Ninety samples of aqueous humor from UM-containing eyes were analyzed using a high-throughput multiplex immunoassay that enables simultaneous analysis of 92 predefined protein biomarkers. Cytokine expression was compared to clinical and histopathological characteristics. Cluster analysis was performed, after which the clusters were compared with clinical and histopathological tumor characteristics.

RESULTS. Cluster analysis revealed three distinct clusters, with one cluster showing hardly any inflammatory cytokines, one showing intermediate levels, and one showing a high expression of inflammation-related biomarkers. Significant differences between the clusters were seen with regard to patient age ($P = 0.008$), tumor prominence ($P = 0.001$), ciliary body involvement ($P < 0.001$), American Joint Committee on Cancer (AJCC) stage ($P < 0.001$), monosomy of chromosome 3 ($P = 0.03$), and gain of chromosome 8q ($P = 0.04$), with the cluster with a highest cytokine expression having the worst prognostic markers. Especially apoptosis-related cytokines were differentially expressed.

CONCLUSIONS. Analysis of cytokines in the aqueous humor shows distinct differences between aqueous humor samples and allocates these samples into three different prognostic tumor clusters. Especially large tumors with ciliary body involvement and monosomy 3 were associated with many cytokines, especially apoptosis-related cytokines. The presence of these cytokines in the aqueous humor may play a role in the lack of effective antitumor immune responses.

Keywords: uveal melanoma, aqueous humor, liquid biopsy, cytokines, immunotherapy

Uveal melanoma (UM) is the most common primary intraocular malignancy in adults, and may develop in the choroid, ciliary body, or iris. While UM accounts for 5% of all malignant melanoma, it accounts for 13% of deaths due to a malignant melanoma.[1] Standard treatment options for the primary tumor comprise radiotherapy ([106]ruthenium or [125]iodine brachytherapy, proton beam therapy, or stereotactic radiation) or surgery (resection or enucleation).[2,3] No systemic therapy has yet been demonstrated to improve survival in the metastatic setting, but this malignancy is potentially an ideal candidate for adjuvant therapy, as several markers are able to accurately predict which patients will develop metastases. Useful parameters include specific chromosome aberrations,[4] mRNA expression patterns,[5] and mutations, such as those in the BRCA1-associated protein 1 (*BAP1*) gene.[6] Immunohistochemical staining for BAP1 protein can also be used for prognostication.[7–9] Loss of chromosome 3, loss of nuclear BAP1

expression, and a class 2 gene expression profile usually occur together.[7,10,11]

Loss of chromosome 3/BAP1 expression is associated with an increased number of lymphocytes and macrophages in primary UM.[12,13] However, the presence of an inflammatory phenotype is linked to a bad and not a good prognosis.

Several studies have shown that a range of different proteins, including cytokines, can be identified in anterior chamber fluid and vitreous.[8,9,14–17] The vitreous fluid of UM-containing eyes showed high concentrations of several inflammatory cytokines and chemokines that correlated predominantly with tumor size, and with the presence of an immune cell infiltrate.[18] These studies did not look at the chromosome status.

Usui et al.[14] compared immune mediators in aqueous humor samples between eyes with a UM and with benign intraocular tumors.[14] Aqueous humor levels of angiogenin, IL-8 (CXCL8), and monocyte chemoattractant protein (MCP)-1 (CCL2) were

significantly higher in eyes with UM compared to the fluid from eyes with different types of benign tumors ($P < 0.05$). Ly et al.[19] observed that aqueous humor samples of UM eyes often showed increased levels of a range of inflammation-related cytokines, when compared to cataract eyes. Increased IL-6 and macrophage migration inhibitory factor (MIF) expression were found to correlate with ciliary body involvement and the presence of an epithelioid cell type, while a high RANTES and vascular endothelial growth factor (VEGF) expression correlated with a large largest basal diameter (LBD) and tumor height. However, none of the cytokine levels were of predictive value for survival.

In order to determine the tumor's chromosome or mRNA status or BAP1 expression for prognostication, one needs to have tumor material, obtained either after enucleation or resection or by taking a biopsy. Success rates of the genetic typing of the tumor vary between 78% and 93%, depending on the surgical technique and tumor location.[20–22] Disadvantages include the need for using an operating room, technical challenges in smaller tumors, and a small but present risk of surgical complications. A liquid biopsy from the anterior chamber is technically less challenging and can be performed as an outpatient procedure, using topical anesthesia. As an inflammatory phenotype is associated with the prognostic parameters monosomy 3 and mRNA class 2,[10] we hypothesized that one can determine the prognostic category of a UM by studying cytokines in the aqueous humor. Furthermore, an analysis of aqueous humor might be used to determine whether a tumor is likely to express immune checkpoint inhibitors, potentially offering a selection method for choosing patients for immunotherapy.[23] Information obtained from a liquid biopsy might therefore be used for prognostication, selection for inclusion in adjuvant trials, or selection for participation in intensified screening programs for early detection of metastases. We set out to determine the presence of a large selection of cytokines in the aqueous humor of UM-containing eyes, obtained by enucleation, and compared their presence with clinical and histological information.

MATERIALS AND METHODS

Study Approval

This project was approved by the Biobank of the LUMC (number: Uveamelanoomlab-2019-4, approval May 2019). The research adhered to Dutch law and the tenets of the Declaration of Helsinki (World Medical Association of Declaration 2013; ethical principles for medical research involving human subjects).

Clinical Characteristics and Histopathological Examination

This study was conducted at the Department of Ophthalmology, Leiden University Medical Center (LUMC), Leiden, The Netherlands. We used 90 samples of aqueous humor that were obtained from 90 patients who underwent enucleation for UM at the LUMC between 1999 and 2016. Clinical data were obtained from medical files and histopathological data from pathology reports (Table 1). Anterior chamber paracentesis was performed immediately after enucleation, by a researcher in the laboratory of Ophthalmology, using a 23-gauge needle, and aqueous humor was frozen at −80°C and stored until the experiment was performed. Following retrieval of aqueous humor, a tumor sample was taken for storage for DNA or mRNA analysis, and the remaining tumor tissue was formalin fixed (4% neutral buffered) for 24 hours and subsequently embedded in paraffin.

Evaluation on hematoxylin- and eosin-stained 4-μm-thick sections included largest basal diameter (LBD, in millimeters), thickness (in millimeters), mitotic count (per 2 mm² at ×40 magnification, counting eight high-power fields), tumor location, and cell type (assessed according to the Armed Forces Institute of Pathology atlas[24]; a "mixed" cell type is defined when spindle and epithelioid cells are both present as at least 5% of tumor cells). Immunohistochemistry (IHC) of BAP1 was performed as previously described, assessed by a pathologist specialized in ophthalmic oncology.[9] Tumors were scored as BAP1 positive or negative according to the nuclear staining, using a mouse monoclonal antibody raised against amino acids 430 to 729 of human BAP1 (clone sc-28383, 1:50 dilution; Santa Cruz Biotechnology, Dallas, TX, USA). Tumors were staged in accordance with the 8th edition of the American Joint Committee on Cancer (AJCC) staging manual.[25] Assessment of the clinical extent of retinal detachment (RD) and the presence of subretinal fluid was evaluated and scored by an experienced clinician using five commonly used categories (from 0 [representing no RD] to 4 [representing complete RD]).[26,27]

For follow-up, we used the period of time between the enucleation date and the last date for which follow-up was available. This information was obtained from the patient's charts and through the Dutch National Registry.[28] The average time of follow-up in the 84 cases was 58 months, and at the end of follow-up, 34 patients were alive (with 18/34 patients having a follow-up of at least 5 years and 16 patients of at least 2 years); 50 patients had passed away—37 died from metastases of UM, and 13 of other causes.

Cytogenetic Analysis of Tumor Material

Genetic information was obtained from the Department of Clinical Genetics at the LUMC, as described before.[28]

Protein Measurement

Proteins were measured in the aqueous humor using the Olink Immuno-Oncology panel (Olink Proteomics AB, Uppsala, Sweden) according to the manufacturer's instructions. The Proximity Extension Assay (PEA) technology has been described,[29] and enables measuring 92 proteins in 90 samples and 6 controls, using 1 μL of each sample, as stated: "pairs of oligonucleotide-labelled antibody probes bind to their targeted protein, and if the two probes are brought in close proximity, the oligonucleotides will hybridize in a pairwise manner. The addition of a DNA polymerase leads to a proximity-dependent DNA polymerization event, generating a unique PCR target sequence. The resulting DNA sequence is subsequently detected and quantified using a microfluidic real-time PCR instrument (Biomark HD, Fluidigm). The final assay read-out is presented in Normalized Protein eXpression (NPX) values, which is an arbitrary unit on a log2-scale where an increased value corresponds to a higher protein expression." All assay validation data (detection limits, intra- and interassay precision data, and so on) are available on the manufacturer's website (www.olink.com; in the public domain). This includes the measuring ranges defined by the lower limit of quantification (LLOQ) and upper limit of qualification (ULOQ).

Data Selection Criteria

We determined the presence of 92 inflammation-related cytokines in anterior chamber fluid of 90 enucleated UM-containing eyes to test whether these cytokines can differentiate between prognostically good and bad UM. A total of 88 samples (98%) passed the quality control test.[30] One sample

TABLE 1. Characteristics of UM Patients Primarily Enucleated in the LUMC Between 1999 and 2016 ($n = 84$), Divided Into Three Clusters, Based on Cytokine Expression in the Aqueous Humor

Clinical and Histopathological Characteristics	Patients, *n* (%)*			
	Cluster 1, *n* = 37	Cluster 2, *n* = 36	Cluster 3, *n* = 11	*P* Value
Sex				0.56†
Females	18 (49)	14 (61)	6 (55)	
Males	19 (51)	22 (39)	5 (46)	
Eye				0.63†
OD	18 (49)	21 (58)	5 (45)	
OS	19 (51)	15 (42)	6 (55)	
Age at enucleation, mean, y (±SD)	55 (±14)	62 (±15)	70 (±11)	0.008§
Eye color, known in 58 cases				0.007†
Light: blue, gray, green, hazel	16 (76)	26 (90)	3 (38)	
Dark: brown	5 (24)	3 (10)	5 (63)	
Largest basal tumor diameter in mm, mean (±SD)	12.2 (±2.7)	12.9 (±2.8)	14.7 (±3.1)	0.04§
Tumor prominence in mm, mean (±SD)	6.4 (±2.8)	8.2 (±2.6)	9.6 (±2.9)	0.001§
Ciliary body involvement				<0.001†
No	32 (87)	20 (56)	3 (27)	
Yes	5 (14)	16 (44)	8 (73)	
Mitotic count‖ mean (±SD)	4.4 (±3.8)	5.1 (±3.0)	7.6 (±9.1)	0.16§
Histopathological cell type				0.048†
Spindle cell	17 (46)	10 (28)	1 (9)	
Epithelioid or mixed cell type	20 (54)	26 (72)	10 (91)	
Pigmentation of the tumor, known in 80 cases				0.57†
None to limited	20 (56)	20 (59)	4 (40)	
Moderate to intense	16 (44)	14 (41)	6 (60)	
Bruch's membrane broken, known in 80 cases				0.21†
Unclear	6 (17)	4 (11)	3 (27)	
Intact	10 (29)	4 (11)	2 (18)	
Broken	18 (53)	27 (77)	6 (54)	
Subretinal fluid				0.38‡
No subretinal fluid	1	1	2	
Subretinal fluid: detachment over and around the melanoma	15	12	1	
Subtle fluid at 6 o'clock and locally within the vascular arcade	13	11	5	
Detachment of two to three quadrants	7	10	1	
Total detachment	1	2	2	
AJCC stage				<0.001‡
I	6 (17)	1 (3)	0 (0)	
IIA	16 (44)	10 (28)	0 (0)	
IIB	9 (25)	11 (31)	2 (18)	
IIIA, IIIB, IIIC	5 (14)	14 (39)	7 (64)	
IV	0 (0)	0 (0)	2 (18)	
Metastases				0.12†
No	23 (62)	18 (50)	3 (27)	
Yes	14 (38)	18 (50)	8 (73)	
Vital status				0.17†
Death due to UM metastases	12 (32)	18 (50)	7 (64)	
Death due to other causes	6 (16)	7 (19)	0 (0)	
Alive at last follow-up date	19 (51)	11 (31)	4 (36)	
Monosomy 3 status, known in 81 cases				0.03†
No	16 (46)	14 (39)	1 (10)	
Yes	19 (54)	22 (61)	9 (90)	
8q status, known in 75 cases				0.04†
No gain of 8q	15 (42)	9 (26)	0 (0)	
Gain of 8q	21 (58)	26 (74)	9 (100)	
BAP1 staining, known in 71 cases				0.18†
Positive	16 (57)	12 (35)	3 (33)	
Negative	12 (43)	22 (65)	6 (67)	

* Percentages are rounded and may not total 100.
† Pearson χ^2 test.
‡ Linear-by-linear association.
§ 1-way ANOVA.
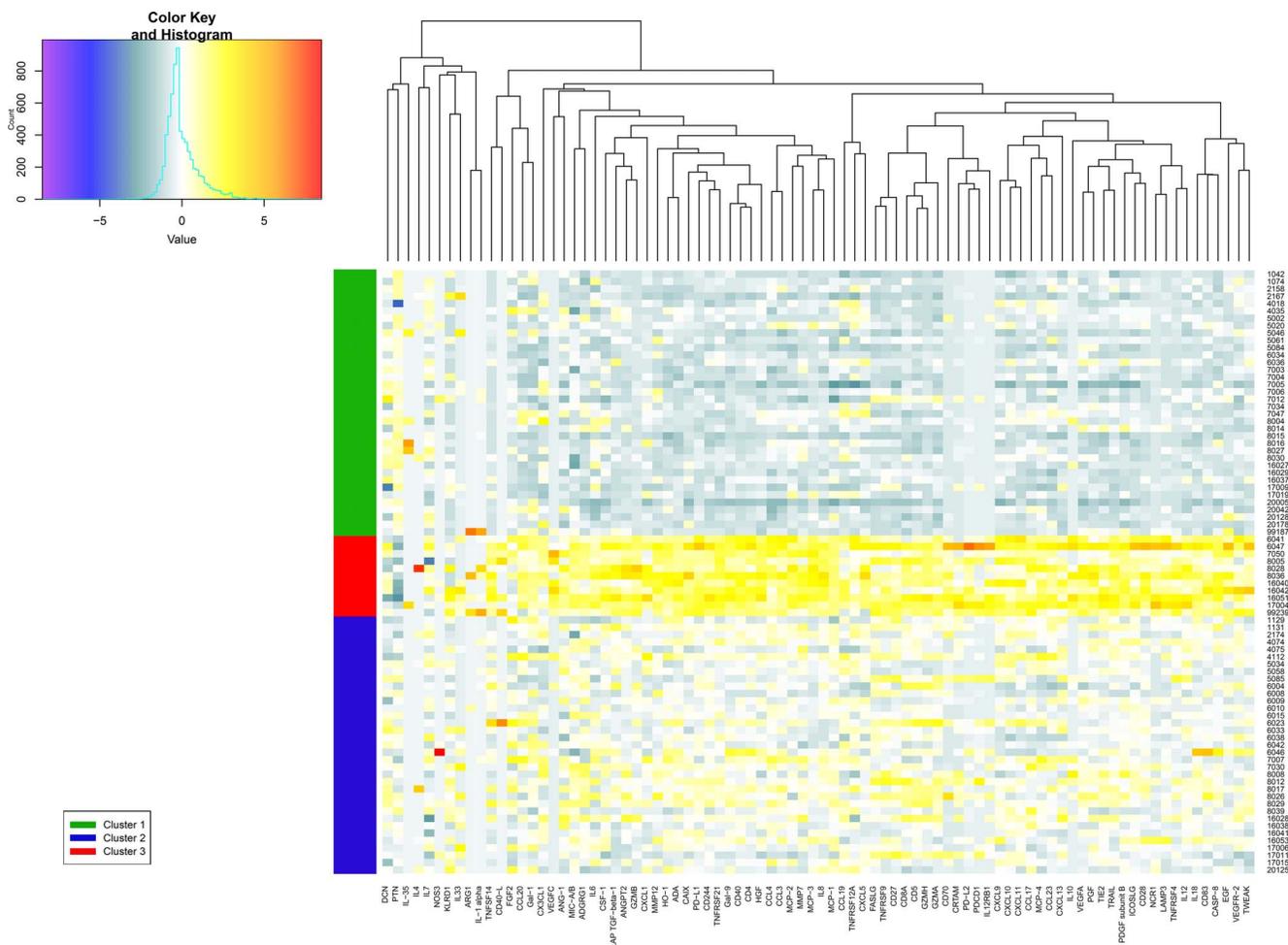‖ *n* mitosis per mm^2 with ×40 magnification and 8 high-power fields.

FIGURE 1. Cluster analysis of 84 aqueous humor samples from UM eyes. Heat map ordered by clustering of 84 aqueous humor samples from UM eyes reveals three distinct clusters, 1 ($n = 37$), 2 ($n = 36$), and 3 ($n = 11$), which are linked to metastatic death due to UM. The heat map shows the supervised clustering where the colors on the *left* represent the three different clusters: Cluster 1 is displayed in *green*, cluster 3 in *red*, and cluster 2 in *blue*.

was removed due to being an exceptional outlier, and one sample due to excessive variability (see Supplementary Fig. S1). In total, samples from 84 eyes were included in the analysis (for characteristics of the tumors see Table 1).

Eight of the 92 biomarkers (IFN-beta, IL2, IL5, IL13, IL-21, CXCL12, IFN-gamma, and TNF) were always below the 5% limit of detection (LOD) and were not studied further. Our analysis therefore included information on 84 biomarkers (see Supplementary Fig. S2).

Statistical Analysis

All clinical, histopathological, and cytogenetic data were collected in an SPSS database. Analyses were subsequently performed using both the statistical programming language R, version 1.14.4 (R Foundation for Statistical Computing, Vienna, Austria), including the packages for data science Tidyverse, Broom, Grepel, and Gplots, and SPSS (IBM SPSS Statistics for Windows, Version 23.0; IBM Corp., Armonk, NY, USA).

Population characteristics were described using medians and percentages. The Pearson χ^2 test was used to analyze categorical data, the Student's *t*-test to compare means between two groups, and analysis of variance (ANOVA) to analyze the significance between the means of more than two groups, for example, the different clusters, including a Tukey's honestly significant difference (HSD) post hoc test.

A volcano plot was made to show significant changes among the biomarkers in relation to tumor characteristics. Kaplan-Meier curves were made and the logrank test was used to analyze significance. Differences were considered to be significant if $P <$ 0.05 after correction for multiple testing, if indicated.

In order to perform a nonsupervised clustering using the 84 samples, the k-means clustering algorithm was used. All assays were scaled using the mean centering with standard deviation (Z-scores), before an unsupervised clustering algorithm was applied. An elbow plot was used to determine the number of underlying clusters (Supplementary Fig. S3). A scatterplot depicting the frequency of positive cytokines among the different AJCC stages was created using UnivarScatter function in MATLAB and Statistics Toolbox Release 2018a (MathWorks, Natick, MA, USA).

RESULTS

Cytokine Expression and Tumor Characteristics

We wondered whether one could take an aqueous humor sample of a UM-containing eye to determine the patient's
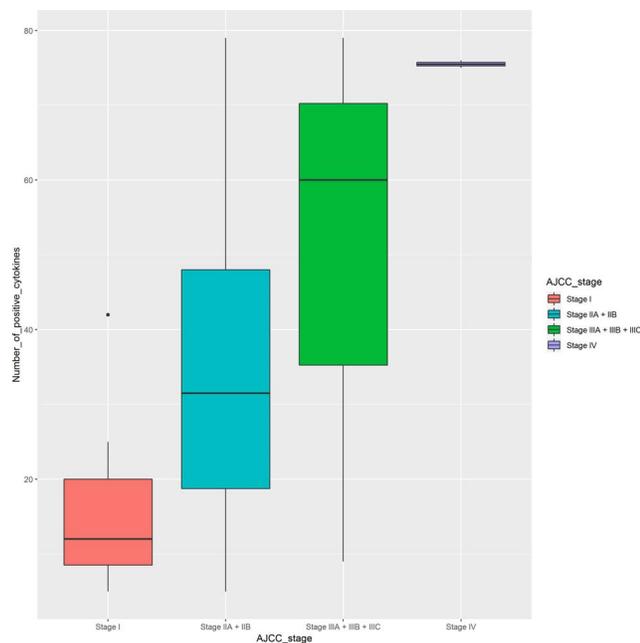
FIGURE 2. Frequency of cytokines with a positive expression (an expression value above the median), displayed per AJCC stage (Kruskal-Wallis test, $P < 0.001$).

prognosis, and whether we could use the presence of cytokines in the anterior chamber to identify specific subgroups of patients. Levels of expression of 84 oncology- and inflammation-related cytokines were determined in the aqueous humor of 84 UM-containing eyes. A heat map of the different samples shows the expression levels of the cytokines in the different samples, indicating a high variability in the number of cytokines present (Fig. 1).

We noticed a positive correlation between the number of positive cytokines and the presence of epithelioid cells (Mann-Whitney U test, $P = 0.006$), histopathological involvement of the ciliary body (Mann-Whitney U test, $P < 0.001$), AJCC stage (Kruskal-Wallis test, $P < 0.001$, Fig. 2) and gain of chromosome 8q (Mann-Whitney U test, $P = 0.019$). The association with monosomy 3 did not reach statistical significance (Mann-Whitney U test, $P = 0.095$).

Cluster Analysis

We determined whether we could find clusters of cases with a similar cytokine expression pattern. Unsupervised clustering provided an optimum of three clusters (see Supplementary Fig. S3). A principal component analysis was performed to visualize the three clusters (Fig. 3). In cluster 1 ($n = 37$), very few cytokines were present in the aqueous humor; cluster 2 ($n = 36$) showed an intermediate number of expressed cytokines. In contrast, cluster 3 ($n = 11$) revealed expression of many cytokines.

The most differentially expressed cytokines among the three clusters were adenosine deaminase (ADA), CD244, CD40, galactin-9 (Gal-9), MCP-3, programmed death-ligand 1 (PD-L1), tumor necrosis factor receptor superfamily 21 (TNFRSF21), and tumor necrosis factor-related apoptosis-inducing ligand (TRAIL).

The three clusters differed significantly in patient age ($P = 0.008$), eye color ($P = 0.007$), LBD ($P = 0.041$), prominence ($P = 0.001$), AJCC stage ($P < 0.001$), ciliary body involvement ($P < 0.001$), cell type ($P = 0.048$), monosomy of chromosome 3 ($P = 0.03$), and amplification of chromosome 8q ($P = 0.04$), with the two clusters with more cytokines showing the worst prognostic markers. Given the inflammatory component of these data, we correlated the presence and extent of exudative retinal detachment to the clusters; we did not find any correlation to the clusters.
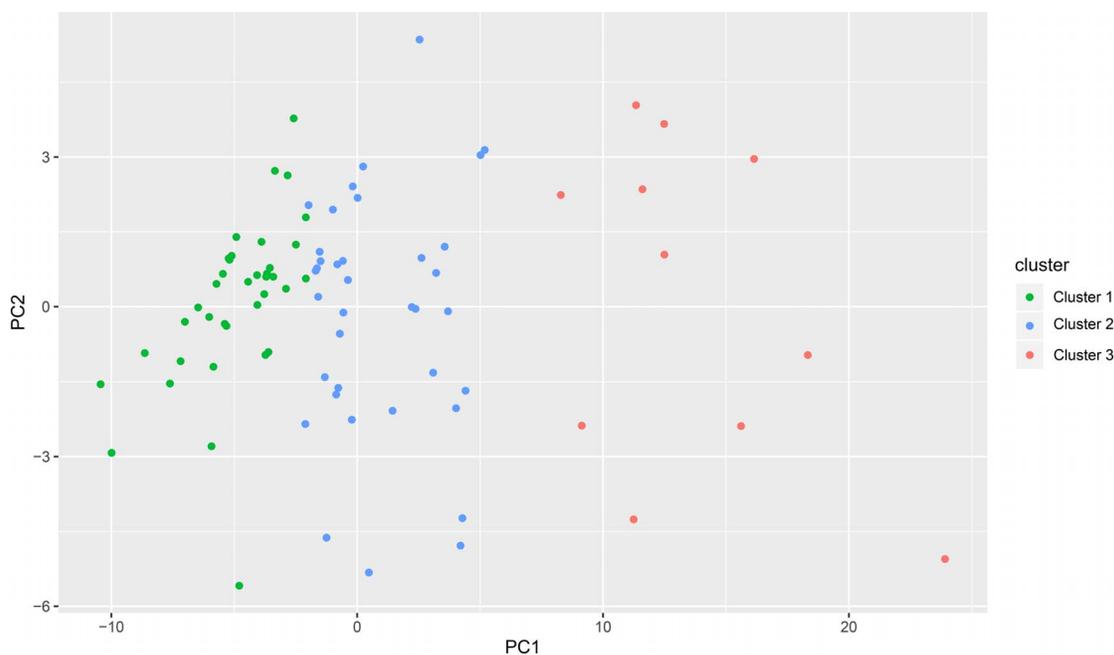

FIGURE 3. Visualization of clusters aided by the principal component analysis. The graph illustrates how the three clusters detected with k-means are separated, with principle component 1 (PC1) explaining 50%, PC2 explaining 6%, and PC3 explaining 4% of variation, indicating that individual higher-order components explain little variance. Cluster 1 is displayed in *green* ($n = 37$), cluster 2 is displayed in *blue* ($n = 36$), and cluster 3 in *red* ($n = 11$).
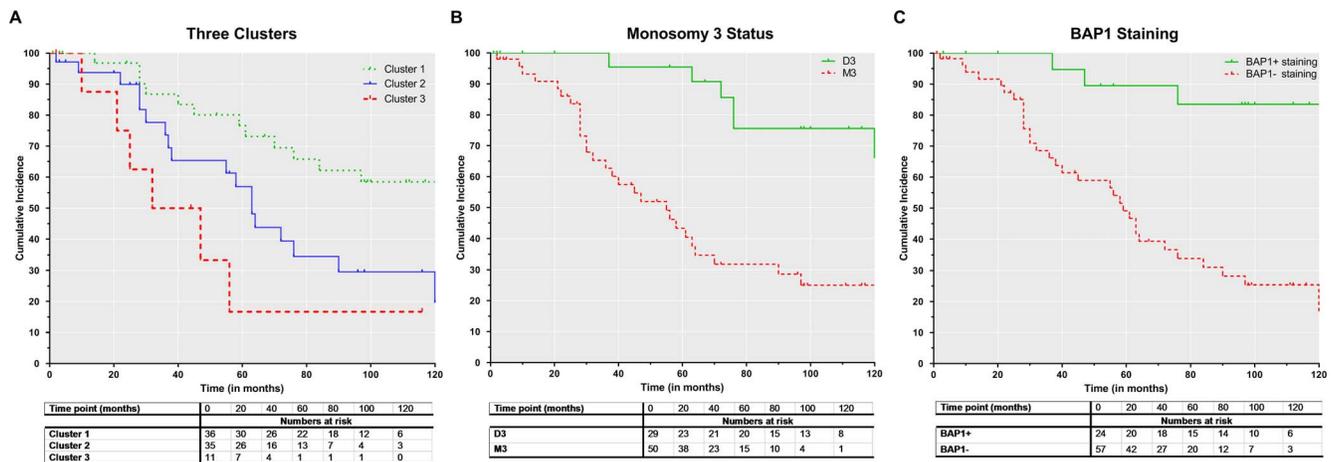
FIGURE 4. (A) Cluster 1 has a better survival than clusters 2 and 3. Survival in cluster 1 differs significantly from cluster 2 (logrank test, $P = 0.02$) and cluster 3 (logrank test, $P = 0.004$). Survival in clusters 2 and 3 does not differ significantly (logrank test, $P = 0.137$). (B) Survival curves of monosomy 3 tumors versus disomy 3 tumors of all tumors involved in this study ($P < 0.01$). (C) Survival curves based on the BAP1 protein expression of all tumors involved in this study ($P < 0.01$).

Characteristics of Cluster 3

The 11 patients in cluster 3 with the highest number of cytokines in the anterior chamber were significantly older at enucleation, with a mean age of 70, in comparison with clusters 1 and 2 (with a mean age of 55 and 62, respectively) (Table 1, 1-way ANOVA, $P = 0.008$). The patients in cluster 3 more often had dark eyes (63%) than patients in clusters 1 and 2 (24% and 10%, respectively) (Pearson χ^2 test, $P = 0.007$).

TABLE 2. Comparison of Clinical, Histopathological, and Chromosomal Characteristics Between the Three Clusters. Significant Results of Multivariate Analysis With Tukey HSD Multiple-Comparison Correction

Characteristic	Clusters Compared	Difference of Mean	Significance
Age at enucleation, mean†			**0.032**
	1, 2	7.98	0.34
	1, 3	17.57*	0.028
	2, 3	9.59	0.14
Eye color†			**0.014**
	1, 2	0.28	0.20
	1, 3	0.12	0.79
	2, 3	0.40*	0.017
Ciliary body involvement†			**<0.001**
	1, 2	0.38	0.09
	1, 3	0.87*	<0.001
	2, 3	0.49*	0.006
Tumor prominence†			**0.015**
	1, 2	0.74	0.70
	1, 3	2.90*	0.027
	2, 3	2.16*	0.028
Gain of 8q†			**0.011**
	1, 2	0.37	0.058
	1, 3	0.58*	0.008
	2, 3	0.37	0.30
AJCC stage†: I/IIAB/IIIABC/IV			**<0.001**
	1, 2	0.68	0.058
	1, 3	1.79*	<0.001
	2, 3	1.11*	<0.001

Bold values indicate statistical significance $P < 0.05$.
* The mean difference is significant at the 0.05 level.
† 1-way MANOVA test with Tukey HSD correction.

The tumors of cluster 3 were significantly larger than tumors in clusters 1 and 2 (mean LBD was 14.7 vs. 12.2 and 12.9 mm, respectively, $P = 0.04$), more often showed an epithelioid or mixed cell type, and more often showed monosomy 3 (90% in cluster 3, vs. 51% and 64% in clusters 1 and 2, respectively, $P = 0.03$, Pearson χ^2 test). Additionally, all tumors in cluster 3 showed gain of 8q, which was significantly more than in cluster 1 or 2 (with 58% and 76%, respectively) ($P = 0.04$, Pearson χ^2 test).

Survival Differences Between the Clusters

A Kaplan-Meijer survival curve of the three clusters showed a significant difference in melanoma-related survival between clusters 1 and 2 (logrank test, $P = 0.02$) and between clusters 1 and 3 (logrank test, $P = 0.004$). There was no significant difference in survival between clusters 2 and 3 (logrank test, $P = 0.14$) (Fig. 4). In cluster 1, 12 out of 18 patient deaths were due to metastatic UM; in cluster 2, 18 out of 25 patients died of metastases, and in cluster 3, all seven deaths were caused by metastatic disease from a UM.

Multivariate Analyses

When using the most significant associations in a multivariate analysis (1-way MANOVA test with Tukey's HSD post hoc correction, details provided in Table 2), we observed that involvement of the ciliary body was the most significant parameter to differentiate between the clusters (with a significance of $P < 0.001$ between clusters 1 and 3).

In a multivariate analysis, eye color remained statistically significant as well: Cluster 3 contained more eyes with brown irises than cluster 2 ($P = 0.017$). Also, the mean age at enucleation remained significantly different between clusters 1 and 3 ($P = 0.028$). When looking at chromosomal abnormalities, a gain of 8q remained significantly different between clusters 1 and 3 ($P = 0.008$).

Cytokines Involved in Apoptosis

Interestingly, out of the most differentially expressed cytokines between the three clusters, four are involved in the process of apoptosis (CD40, Gal-9, TNFRSF21, and TRAIL). TNFRSF9 was the only cytokine that was linked to both chromosome 8q and chromosome 3. This implies a potential role for apoptosis-

related cytokines in prognostically unfavorable UM. When looking at the association between the presence of these biomarkers and survival, we observed no significant difference in survival between low and high levels of TRAIL (logrank, $P = 0.069$).

However, we did find significant differences in survival when looking at low versus high levels of CD40 (logrank, $P = 0.007$), Gal-9 (logrank, $P = 0.011$), TNFRSF9 (logrank, $P = 0.014$) and TNFRSF21 (logrank, $P = 0.005$), and FASLG (logrank, $P = 0.011$) with high levels being expressed in the aqueous humor of tumors with the worst survival.

DISCUSSION

To determine whether one can use a liquid biopsy in order to discriminate between high- and low-risk UM, we analyzed the presence and quantity of 84 proteins related to oncology or immunology in aqueous humor samples of 84 UM-containing eyes. A cluster analysis based on cytokine expression identified three clusters, which revealed significant differences when compared to clinical, histopathological, and chromosomal characteristics. While most tumors in cluster 3 had monosomy 3 and all had a gain of 8q, we found that involvement of the ciliary body was of more importance in differentiating between the three clusters than chromosome status or tumor size. The close association between the ciliary body and the anterior chamber may provide an anatomic explanation. De Lange et al.[30] and Singh et al.[31] demonstrated that 8q is an early chromosomal change in the development of UM. Gezgin et al.[12] recently showed that tumors with disomy 3 and extra copies of 8q already displayed an inflammatory phenotype.

The cluster analysis led to some new insights into tumor biology. When comparing the cytokines between the groups, it was noticed that many of the most differentially expressed cytokines were related to apoptosis. TRAIL, also known as Apo2L, is part of the *TNF* gene superfamily that has the capacity to induce apoptosis. TRAIL has been recognized as a therapeutic modality via TRAIL-induced apoptosis. When we looked at the survival and compared cases with low and high TRAIL levels in the aqueous humor, survival did not differ significantly.

Another important inducer of apoptosis is FASLG: We found that FASLG expression in the aqueous humor was related to survival, with high levels corresponding to poor survival. A prior study analyzed the TCGA database and found that high mRNA levels of FASLG in the tumor were associated with a significantly worse prognosis ($P < 0.001$).[32] A study by Zhu et al.[32] suggested that FASLG expression is associated with T-cell infiltrate.

Galactin-9 has been identified as a clinical predictor in UM.[33] Also, Gal-9 has been studied in tumor material and plasma of patients with metastatic melanoma. It is thought that Gal-9 promotes the alternatively activated macrophage M2 phenotype.[34] When looking at levels of Gal-9 in the aqueous humor in relation to survival, we found that high levels of Gal-9 were significantly related to a worse survival (logrank, $P = 0.015$). Also, Gal-9 in the aqueous humor significantly corresponded to expression of the immune checkpoint inhibitor PD-L1 in the aqueous humor (Spearman correlation, $n = 84$, $P < 0.001$). This corresponds to the significant relation between Gal-9 and PD-L1 expression in the tumor, as was found using the TCGA database.[33]

While in our study high levels of Gal-9 correspond to a worse survival, a study analyzing the TCGA UM cohort found that patients with a lower expression of Gal-9 in the tumor had worse survival rates.[35] We hypothesize that high levels of Gal-9 in the anterior chamber of prognostically bad UM is

plausible as expression of Gal-9 is stimulated in a proinflammatory environment,[36] which is the case in UM with an inflammatory phenotype.[37,38] Galactin-9 has been proven to impair the function of NK cells[39] as well as leading to influx of forkhead box P3 (FOXP3) positive regulatory T-cells, which are independent predictors of worse survival in UM.[36,38] All these data indicate the presence of a wide range of molecules in the anterior chamber that have immunosuppressive qualities.

A strong point in this study is that the assay requires only 1 μL aqueous humor, an amount that can be obtained in an outpatient setting. Studies in other ocular malignancies have already demonstrated that aqueous humor can serve as a surrogate tumor biopsy for analyses, such as the detection of cell-free DNA for genetic analysis in retinoblastoma and the measurement of IL-10 levels as a biomarker for intraocular lymphoma.[40–42]

The ciliary body is specifically listed as a parameter in differentiating prognostic categories in the *Cancer Staging Manual* of the AJCC for staging ciliary body and choroidal melanoma.[43] A reason for the high expression of cytokines in the anterior chamber fluid of cluster 3 tumors could be the anatomic involvement of the ciliary body, which produces the aqueous humor. Uveal melanomas with involvement of the ciliary body are more aggressive tumors, and may cause more cell turnover and cell death, leading to more leakage of inflammatory mediators.

In conclusion, we observed a large variation in the presence of a wide range of cytokines in the aqueous humor of UM-containing eyes, leading to the identification of three clusters, which differ with regard to patient age, AJCC category, ciliary body involvement, and chromosome 8q amplification, supporting the previous finding of an association between chromosome 8q amplification and inflammation.[12]

References

1. Berus T, Halon A, Markiewicz A, Orlowska-Heitzman J, Romanowska-Dixon B, Donizy P. Clinical, histopathological and cytogenetic prognosticators in uveal melanoma - a comprehensive review. *Anticancer Res*. 2017;37:6541–6549.

2. Amaro A, Gangemi, R, Piaggio F, et al. The biology of uveal melanoma. *Cancer Metastasis Rev*. 2017;36:109–140.

3. Dogrusoz M, Jager MJ, Damato B. Uveal melanoma treatment and prognostication. *Asia Pac J Ophthalmol (Phila)*. 2017;6: 186–196.

4. Dogrusoz M, Jager MJ. Genetic prognostication in uveal melanoma. *Acta Ophthalmol*. 2018;96:331–347.

5. Onken MD, Worley LA, Ehlers JP, Harbour JW. Gene expression profiling in uveal melanoma reveals two molecular classes and predicts metastatic death. *Cancer Res*. 2004;64: 7205–7209.

6. Harbour JW, Onken MD, Roberson ED, et al. Frequent mutation of BAP1 in metastasizing uveal melanomas. *Science*. 2010;330:1410–1413.

7. van Essen TH, van Pelt SI, Versluis M, et al. Prognostic parameters in uveal melanoma and their association with BAP1 expression. *Br J Ophthalmol*. 2014;98:1738–1743.

8. Kalirai H, Dodson A, Faqir S, Damato BE, Coupland SE. Lack of BAP1 protein expression in uveal melanoma is associated with increased metastatic risk and has utility in routine prognostic testing. *Br J Cancer*. 2014;111:1373–1380.

9. Koopmans AE, Verdijk RM, Brouwer RW, et al. Clinical significance of immunohistochemistry for detection of BAP1 mutations in uveal melanoma. *Mod Pathol*. 2014;27:1321–1330.

10. Robertson AG, Shih J, Yau C, et al. Integrative analysis identifies four molecular and clinical subsets in uveal melanoma. *Cancer Cell*. 2018;33:151.

11. Grossniklaus HE. Understanding uveal melanoma metastasis to the liver: the Zimmerman effect and the Zimmerman hypothesis. *Ophthalmology*. 2019;126:483–487.

12. Gezgin G, Dogrusoz M, van Essen TH, et al. Genetic evolution of uveal melanoma guides the development of an inflammatory microenvironment. *Cancer Immun Immunother*. 2017;66:903–912.

13. Maat W, Ly LV, Jordanova ES, et al. Monosomy of chromosome 3 and an inflammatory phenotype occur together in uveal melanoma. *Invest Ophthalmol Vis Sci*. 2008;49:505–510.

14. Usui Y, Tsubota K, Agawa T, et al. Aqueous immune mediators in malignant uveal melanomas in comparison to benign pigmented intraocular tumors. *Graefes Arch Clin Exp Ophthalmol*. 2017;255:393–399.

15. Cheng Y, Feng J, Zhu X, Liang J. Cytokines concentrations in aqueous humor of eyes with uveal melanoma. *Medicine*. 2019;98:e14030.

16. Dunavoelgyi R, Funk M, Sacu S, et al. Intraocular activation of angiogenic and inflammatory pathways in uveal melanoma. *Retina*. 2012;32:1373–1384.

17. Boyd SR, Tan D, Bunce C, et al. Vascular endothelial growth factor is elevated in ocular fluids of eyes harbouring uveal melanoma: identification of a potential therapeutic window. *Br J Ophthalmol*. 2002;86:448–452.

18. Nagarkatti-Gude N, Bronkhorst IH, van Duinen SG, Luyten GP, Jager MJ. Cytokines and chemokines in the vitreous fluid of eyes with uveal melanoma. *Invest Ophthalmol Vis Sci*. 2012;53:6748–6755.

19. Ly LV, Bronkhorst IHG, van Beelen E, et al. Inflammatory cytokines in eyes with uveal melanoma and relation with macrophage infiltration. *Invest Ophthalmol Vis Sci*. 2010;51:5445–5451.

20. Angi M, Kalirai H, Taktak A, et al. Prognostic biopsy of choroidal melanoma: an optimised surgical and laboratory approach. *Br J Ophthalmol*. 2017;101:1143–1146.

21. Sellam A, Desjardins L, Barnhill R, et al. Fine needle aspiration biopsy in uveal melanoma: technique, complications, and outcomes. *Am J Ophthalmol*. 2016;162:28–34.

22. Singh AD, Medina CA, Singh N, Aronow ME, Biscotti CV, Triozzi PL. Fine-needle aspiration biopsy of uveal melanoma: outcomes and complications. *Br J Ophthalmol*. 2016;100:456–462.

23. Wierenga APA, Cao J, Luyten GPM, Jager MJ. Immune checkpoint inhibitors in uveal and conjunctival melanoma. *Int Ophthalmol Clin*. 2019;59:53–63.

24. Font RL, Croxatto JO, Rao NA. *Tumors of the Eye and Ocular Adnexa. AFIP Atlas of Tumor Pathology: Series 4*. Silver Spring, MD: The American Registry of Pathology; Armed Forces Institute of Pathology; 2006:56–60.

25. Amin MB, Gress DM, Meyer Vega LR, et al. *AJCC Cancer Staging Manual*. 8th ed. Chicago, IL: American College of Surgeons; 2018.

26. Kivelä T, Eskelin S, Mäkitie T, Summanen P. Exudative retinal detachment from malignant uveal melanoma: predictors and prognostic significance. *Invest Ophthalmol Vis Sci*. 2001;42:2085–2093.

27. Muller K, Nowak PJ, de Pan C, et al. Effectiveness of fractionated stereotactic radiotherapy for uveal melanoma. *Int J Radiat Oncol Biol Phys*. 2005;63:116–122.

28. Dogrusoz M, Bagger M, van Duinen SG, et al. The prognostic value of AJCC staging in uveal melanoma is enhanced by adding chromosome 3 and 8q status. *Invest Ophthalmol Vis Sci*. 2017;58:833–842.

29. Assarsson E, Lundberg M, Holmquist G, et al. Homogenous 96-plex PEA immunoassay exhibiting high sensitivity, specificity, and excellent scalability. *PLoS One*. 2014;9:e95192.

30. de Lange MJ, van Pelt SI, Versluis M, et al. Heterogeneity revealed by integrated genomic analysis uncovers a molecular switch in malignant uveal melanoma. *Oncotarget*. 2015;6:37824–37835.

31. Singh AD, Shields CL, Shields JA. Prognostic factors in uveal melanoma. *Melanoma Res*. 2001;11:255–263.

32. Zhu J, Powis de Tenbossche CG, Cané S, et al. Resistance to cancer immunotherapy mediated by apoptosis of tumor-infiltrating lymphocytes. *Nat Commun*. 2017;8:1404.

33. Basile MS, Mazzon E, Russo A, et al. Differential modulation and prognostic values of immune-escape genes in uveal melanoma. *PLoS One*. 2019;14:e0210276.

34. Enninga EAL, Nevala WK, Holtan SG, Leontovich AA, Markovic SN. Galectin-9 modulates immunity by promoting Th2/M2 differentiation and impacts survival in patients with metastatic melanoma. *Melanoma Res*. 2016;26:429–441.

35. Zhou X, Sun L, Jing D, et al. Galectin-9 expression predicts favorable clinical outcome in solid tumors: a systematic review and meta-analysis. *Front Physiol*. 2018;9:452.

36. Gieseke F, Kruchen A, Tzaribachev N, Bentzien F, Dominici M, Müller I. Proinflammatory stimuli induce galectin-9 in human mesenchymal stromal cells to suppress T-cell proliferation. *Eur J Immunol*. 2013;43:2741–2749.

37. Bronkhorst IH, Vu TH, Jordanova ES, Luyten GP, Burg SH, Jager MJ. Different subsets of tumor-infiltrating lymphocytes correlate with macrophage influx and monosomy 3 in uveal melanoma. *Invest Ophthalmol Vis Sci*. 2012;53:5370–5378.

38. Mougiakakos D, Johansson CC, Trocme E, et al. Intratumoral forkhead box P3-positive regulatory T cells predict poor survival in cyclooxygenase-2-positive uveal melanoma. *Cancer*. 2010;116:2224–2233.

39. Golden-Mason L, McMahan RH, Strong M, et al. Galectin-9 functionally impairs natural killer cells in humans and mice. *J Virol*. 2013;87:4835–4845.

40. Uner OE, Ulrich BC, Hubbard G. Potential of aqueous humor as a surrogate tumor biopsy for retinoblastoma. *JAMA Ophthalmol*. 2018;136:597–598.

41. Berry JL, Xu L, Murphree A, et al. Potential of aqueous humor as a surrogate tumor biopsy for retinoblastoma. *JAMA Ophthalmol*. 2017;135:1221–1230.

42. Cassoux N, Giron A, Bodaghi B, et al. IL-10 measurement in aqueous humor for screening patients with suspicion of primary intraocular lymphoma. *Invest Ophthalmol Vis Sci*. 2007;48:3253–3259.

43. Kivelä T, Kujala E. Prognostication in eye cancer: the latest tumor, node, metastasis classification and beyond. *Eye (Lond)*. 2013;27:243–252.